

Updating the σ - T relationship for galaxy clusters

Xiang-Ping Wu¹, Li-Zhi Fang² and Wen Xu²

¹Beijing Astronomical Observatory, Chinese Academy of Sciences, Beijing 100012, China

²Department of Physics, University of Arizona, Tucson, AZ 85721, USA

Received 15 October, 1997; accepted 13 August, 1998

Abstract. ¹

The relationship between the X-ray determined temperature T of the intracluster gas and the optical measured velocity dispersion σ of the cluster galaxies is often believed to be not only a straightforward but also robust test for the dynamical properties of galaxy clusters. Here, we present the σ - T relationship using the 94 clusters drawn from the largest sample of 149 clusters in literature, for which both σ and T are observationally determined. Employment of the doubly weighted orthogonal distance regression to our sample yields $\sigma = 10^{2.47 \pm 0.06} T^{0.67 \pm 0.09}$, indicating an apparent deviation of dynamical state from that predicted by the isothermal and hydrostatic equilibrium model for galaxy clusters, though the average ratio β_{spec} of specific energy in galaxies to that in gas is found to be in excellent agreement with unity. It shows that a non-isothermal gas distribution with a mean polytropic index of $\gamma = 1.3$ can account for the reported σ - T relationship, while overall clusters can still be regarded as dynamically-relaxed systems.

Key words: galaxies: clustering: general – X-rays: galaxies

1. Introduction

Clusters of galaxies are the largest coherent and gravitationally bound objects in the universe. They are often used for cosmological test of theories of formation and evolution of structures in the universe (e.g. Bahcall & Cen 1993). They also play a potentially important role in the direct measurement of the present mean mass density of the universe (e.g. Bahcall, Lubin & Dorman 1995). Yet, these cosmological applications are closely connected with the question of how reliable our current knowledge about the dynamical properties of clusters would be. Numerous recent observations made primarily at X-ray wave-

band suggest that the gross dynamical properties of galaxy clusters have experienced little evolution since redshift $z \sim 0.8$ (e.g. Mushotzky & Scharf 1997; Rosati et al. 1998; Vikhlinin et al. 1998). A statistical comparison of different cluster mass estimators from optical/X-ray and gravitational lensing measurements shows that, regardless of the presence of substructures and local dynamical activities, overall clusters of galaxies even at intermediate redshift can be regarded as dynamically-relaxed systems (e.g. Allen 1998; Wu et al 1998 and references therein). This essentially justifies the employment of hydrostatic equilibrium for galaxy clusters.

One simpler and more straightforward approach to testing the dynamical state of clusters of galaxies, which was suggested two decades ago (Cavaliere & Fusco-Femiano 1976), is to use the relationship between the X-ray determined temperature T of the intracluster gas and the optical measured velocity dispersion σ of the cluster galaxies: If both galaxies and gas are the tracers of the depth and shape of a common gravitational potential, we would expect $\sigma \sim T^{0.5}$. In other words, the disagreement between the observed σ - T relationship and the expectation of $\sigma \sim T^{0.5}$ may be considered to be a strong indicator for the departure of cluster dynamical state from the isothermal hydrostatic equilibrium. With the rapid growth of optical/X-ray data for clusters of galaxies over the past years, a number of authors (see Table 2) have made attempt at determining the σ - T relationship from various cluster samples. While the resultant σ - T profiles are not inconsistent with $\sigma \sim T^{0.5}$, one cannot exclude the possibility that there is a real deviation of the observed σ - T relationship from that expected under the scenario of isothermal hydrostatic equilibrium. For instance, based on the well-defined cluster samples in which the measurement errors are well determined, Bird, Mushotzky & Metzler (1995), Girardi et al (1996) and White, Jones & Forman (1997) found $\sigma \sim T^{0.6}$. Yet, a difficulty with these determinations arises from the too small cluster samples, which often have large data scatters in the fit of σ - T relationship. It appears that a larger cluster sample is needed in order to achieve a better statistical significance, with which one can determine whether there is an intrinsic dispersion in

Send offprint requests to: X. P. Wu

¹ Table 1 is only available in electronic form at the CDS via anonymous ftp to cdsarc.u-strasbg.fr (130.79.128.5) or via <http://cdsweb.u-strasbg.fr/Abstract.html>

Table 1. Cluster sample (see CDS)

the σ - T relationship due to different physical mechanisms among different clusters. We wish to fulfill the task in the present paper by updating the σ - T relationship for clusters, making use of all the published data sets of σ and T in literature. We examine the question whether the σ - T relationship can be used for the purpose of testing the dynamical properties of clusters.

2. Sample

By extensively searching literature, we find 517 galaxy clusters for which the velocity dispersions (367 clusters) and/or temperatures (299 clusters) are observationally determined. Here we exclude those clusters whose σ or T are obtained by indirect methods such as the L_x - σ and L_x - T correlations (e.g. Ebeling et al. 1996; White et al. 1997) where L_x is the X-ray luminosity, or by the gravitational lensing analysis (e.g. Sadat, Blanchard & Oukbir 1998). The final sample in which both T and σ are available for each cluster contains 149 clusters (Table 1). This compares with the similar but the largest cluster sample (207 clusters) heretofore published by White et al (1997), in which 83 clusters have the measured σ and T , thus we have increased the data set by 66 clusters. Since the data of σ and T are collected among a large number of individual sources, it may be too tedious to list all the references in the present paper. For the majority of the data the reader is referred to Zabludoff, Huchra & Geller (1990), Struble & Rood (1991), Edge & Stewart (1991), Lubin & Bahcall (1993), Gioia & Luppino (1994), White & Fabian (1995), Ebeling et al.(1996), Carlberg et al. (1996), Fadda et al. (1996), Girardi et al. (1996), Girardi et al. (1997), Smail et al. (1997), Mushotzky & Scharf (1997), Wu & Fang (1997), Ettori, Fabian & White (1997) and White et al. (1997).

3. The σ - T relationship

Fig.1 shows velocity dispersion σ versus temperature T for the 149 clusters listed in Table 1, and it is clearly seen that there is a strong correlation between the two variables. Since not all the measurement uncertainties in σ and T are known in our cluster sample, we first employ the standard ordinary least-square (OLS) fit of a power-law to all the data set, which yields

$$\sigma = 10^{2.54 \pm 0.03} T^{0.56 \pm 0.04}, \quad (1)$$

where (also hereafter) σ and T are in units of km s^{-1} and keV, respectively. Note that the error bars in eq.(1) do not include the measurement uncertainties. We then

use the orthogonal distance regression (ODR) technique ODRPACK (Bogg et al. 1989; Bogg & Rogers 1990; Feigelson & Babu 1992) to fit a subsample of 94 clusters, for which the measurement uncertainties in both variables are observationally given (Fig.2). The doubly weighted ODR σ - T relationship reads

$$\sigma = 10^{2.47 \pm 0.06} T^{0.67 \pm 0.09}. \quad (2)$$

Here the quoted 1σ standard deviations are determined by the Monte-Carlo simulation which has taken the measurement uncertainties in both σ and T into account. It turns out that at about 95% confidence interval, we have detected a deviation of the σ - T relationship from that expected in the framework of isothermal and hydrostatic equilibrium for clusters of galaxies, although the parameter scatters are only slightly reduced as compared with the recent result of White et al. (1997).

Nevertheless, as it has been noticed before (Bird et al. 1995), the resultant σ - T relationships seem to depend also on the adopted linear regression methods: The OLS method often provides a relatively smaller power index in the fit than other regression methods such as the Bisector and ODR, which is independent of whether the data are weighted or not. For instance, employing the unweighted ODR method to the whole data set of 149 clusters without including the measurement uncertainties, we can still reach a power-law of large index:

$$\sigma = 10^{2.47 \pm 0.03} T^{0.67 \pm 0.04}. \quad (3)$$

in contrast with the result of eq.(1) obtained by OLS. Indeed, one may arrive at very different conclusions regarding the dynamical properties of clusters based on the different fitting methods. This accounts for the early claim by Lubin & Bahcall (1993), in terms of their fitted relationship $\sigma \propto T^{0.5}$ by OLS, that the overall clusters can be regarded as well virialized and isothermal systems. So, we may need to have a close examination of the working hypotheses in the two fitting methods. Isobe et al. (1990) listed four assumptions under which OLS method may hold. One of them requires that the values of the independent variable (i.e. T in our problem) are measured without error. Namely, in the linear fit of the σ - T relationship, OLS ignores the scatters around T and only minimizes the residuals in σ . On the other hand, ODR method is advocated to deal with the following question (Feigelson & Babu 1992): What is the intrinsic relationship between properties X and Y in these objects, without treating one variable differently from the other? In other words, ODR makes an attempt at accounting for data scatters around both T and σ for our particular problem. Therefore, it appears that in principle OLS cannot be used in the fitting of the σ - T relationship for clusters, in which both σ and T contain significant measurement uncertainties in addition to their intrinsic scatters.

We now examine whether the σ - T relationship evolves with cosmic epoch. To this end, we divide our cluster sam-

at high redshift $z \geq 0.1$. The best OLS fitted σ - T relationships for these two subsamples are

$$\begin{aligned} \sigma &= 10^{2.57 \pm 0.03} T^{0.49 \pm 0.05}, & z < 0.1; \\ \sigma &= 10^{2.57 \pm 0.08} T^{0.56 \pm 0.09}, & z \geq 0.1. \end{aligned} \quad (4)$$

So, within 1σ error bars there is no apparent change in the σ - T relationship between the low-redshift subsample and the high-redshift one. This is consistent with the recent result of Mushotzky & Scharf (1997) based on 13 high-redshift clusters at $z > 0.14$ whose σ and T are well measured. Contrary to the fitting of the σ - T relationship, the study of whether the σ - T relationship varies with redshift is insensitive to the adopted linear regression method as long as we use the same fitting technique. Yet, the actual reason why we did not apply the ODR method to our subsample to do the above exercise is the sparse data of the high-redshift clusters. Nevertheless, a visual examination of Fig.2 reveals that the distributions of the high and low redshift clusters over the σ - T plot do not exhibit significant differences.

Table 2. Summary of the best fitted σ - T relationships

Fig. 1. The σ - T relationship for the 149 clusters in Table 1. The low-redshift ($z < 0.1$) and high-redshift ($z \geq 0.1$) clusters are represented by the open triangles (110) and the filled squares (39), respectively. The solid line is the best OLS fitted relationship to the data.

Fig. 2. The σ - T relationship of the 94 clusters for which the measurement uncertainties in both σ and T are known. The solid line shows the best OLS fit to the data, and the dashed line is the doubly weighted ODR result.

4. The β parameter

An equivalent parameter that has been frequently used to characterize the dynamical properties of clusters is the ratio of specific kinetic energy in galaxies to that in gas:

$$\beta_{spec} \equiv \frac{\sigma^2}{kT/\mu m_p}, \quad (5)$$

where $\mu m_p \approx 0.59$ is the average particle mass. In the framework of the standard isothermal hydrostatic model for clusters, it is expected that $\beta_{spec} = 1$. Fig.3 shows the resulting β_{spec} from the observed σ and T of each cluster listed in Table 1, and the mean value is $\langle \beta_{spec} \rangle = 1.00 \pm 0.52$, indicative of a perfect energy equipartition between the galaxies and gas in clusters. This value is also consistent with the result found from the recent N-body/gasdynamical simulations of formation and evolution of X-ray clusters (Eke, Navarro & Frenk 1998). Because there is an apparent asymmetry in the distribution of the β_{spec} values in Fig.3, we also provide the median and 90% limits of the distribution: $\beta_{spec} = 0.80_{-0.52}^{+1.04}$.

As an analogy to eq.(4), Fig.4 gives another way to demonstrate if clusters have undergone a significant evolution: the mean value β_{spec} versus redshift. It appears that the whole data set is consistent with a nonevolutionary scenario, though there is a scarcity of high-redshift clusters in the present sample. Our doubly weighted ODR relationship reads

$$\beta_{spec} = 10^{0.00 \pm 0.09} (1+z)^{0.10 \pm 0.86}. \quad (6)$$

5. Discussion

ple of 149 clusters into two subsamples according to redshifts: 110 clusters at low redshift $z < 0.1$ and 39 clusters

There are many mechanisms that can lead the σ - T relationship of galaxy clusters to deviate from that predicted

Fig. 3. The parameter $\beta_{spec} = \sigma^2/(kT/\mu m_p)$ for the 149 clusters in Table 1. The dotted line shows the mean value $\langle\beta_{spec}\rangle=1.00$.

Fig. 4. The binned value β_{spec} is plotted against redshift. Each redshift bin except the last point (9 clusters) at large redshift contains 10 clusters.

by the isothermal and hydrostatic equilibrium model. These include the anisotropy of galaxy velocity dispersion σ , the protogalactic winds which heat the intracluster medium, the velocity bias between galaxies and dark matter particles, the asymmetric mass distributions (Bird et al. 1995; Girardi et al. 1996) and the effect of cooling flows (White et al. 1997). Here, we explore another possibility: The intracluster gas is nonisothermal and the gas temperature declines with outward radius. This is primarily motivated by the recent spatially resolved X-ray spectroscopic measurements of many clusters, which show a significant radial temperature decline at large radii (e.g. Briel & Henry 1994; Henriksen & White III 1996; Markevitch et al. 1997; etc). We drop the isothermal assumption but maintain the hydrostatic equilibrium model for clusters. The last point is justified by a number of numerical and observational studies which indicate that on average, galaxy clusters are regular objects with little cosmological and dynamical evolution within $z \approx 1$. The following exercise is to demonstrate how a similar relationship to the observationally fitted one in the present paper, $\sigma \propto T^{0.67}$, is obtained in the framework of nonisothermal gas distribution.

We use a polytropic temperature profile $T = T_0[n(r)/n_0]^{\gamma-1}$ and a conventional β model with $\beta_{fit} = 2/3$ for the gas distribution $n(r) = n_0[1 + (r/r_c)^2]^{-3\beta_{fit}/2}$, where n_0 and r_c are the central gas number density and the core radius, respectively. Strictly speaking, a β model of $\beta_{fit} = 2/3$ corresponds to a polytropic index of $\gamma = 1$ (Cowie, Henriksen & Mushotzky 1987). Our choice of the density profile with $\beta_{fit} = 2/3$ is only to parameterize the observed characteristics. If the X-ray emission of a cluster is detected over a circular aperture of radius r_{cut} from the cluster center due to the limitation of instruments, we would expect an emission-weighted temperature $T_{weighted}$ instead of the temperature profile $T(r)$ when the spatially resolved spectroscopy is not available:

$$T_{weighted} = \frac{\int_0^{r_{cut}} \alpha(T) T n^2(r) r^2 dr}{\int_0^{r_{cut}} \alpha(T) n^2(r) r^2 dr}, \quad (7)$$

where $\alpha(T)$ is cooling function and can be approximately taken to be $\alpha \propto T^{1/2}$ for the thermal bremsstrahlung radiation. r_{cut} corresponds to the edge of the X-ray surface brightness $S(r)$ that the detector can reach:

$$S(r_{cut}) \propto \int_{r_{cut}}^{\infty} \alpha(T) n^2(r) \frac{r dr}{\sqrt{r^2 - r_{cut}^2}}. \quad (8)$$

Similarly, the observed velocity dispersion of cluster galaxies is the so-called average line-of-sight velocity dispersion weighted by the galaxy surface number density profile over a certain aperture. However, unlike the X-ray emitting gas, the spatial distribution of galaxies is more concentrated toward the cluster center and their radial velocity dispersions exhibit no significant decline at the corresponding radius (e.g. Carlberg, Yee & Ellingson 1997). For simplicity, the velocity dispersion of galaxies is assumed to be constant.

We estimate the gas temperature $T = T_c$ at $r = 1.25r_c$ using $T_c = (\mu m_p)\sigma^2$ so that the amplitude of $T(r)$ can be fixed when the polytropic index γ is specified. This choice is somewhat arbitrary. Our main consideration is to ensure that the theoretically expected emission-weighted temperature $T_{weighted}$ is essentially consistent with the observationally determined one T_{obs} . Namely, the position of $r = 1.25r_c$ is determined by requiring $\langle T_{weighted} \rangle = \langle T_{obs} \rangle$ on average for the 94 clusters in Fig.2 (see also Fig.5), in which we take a mean value of the polytropic index, $\gamma = 1.3$, for all the clusters according to the recent measurements of 30 nearby clusters by Markevitch et al. (1998) as well as some theoretical considerations (Chiueh & Wu 1998). If clusters are selected above the same threshold $S(r_{cut})$, r_{cut} can be found for each cluster of different temperature $T(r)$, where an absolute calibration is needed in order to test the correlation between the velocity dispersion σ and the emission-weighted temperature $T_{weighted}$ within $r = r_{cut}$. We adopt such a calibration that for a central temperature $T_0 = 5$ keV cluster, $r_{cut} = 2r_c$. We utilize the data set of velocity dispersion in the subsample of 94 clusters, in which the measurement uncertainties

Fig. 5. Comparison of the theoretically estimated gas temperature $T_{weighted}$ in terms of eqs.(7) and (8) with the observationally determined value T_{obs} for a subsample of 94 clusters shown in Fig.2. A β density profile with $\beta_{fit} = 2/3$ and a polytropic temperature distribution with $\gamma = 1.3$ are used. Absolute calibrations are made through $T(1.25r_c) = (\mu m_p)\sigma^2$ and $T_0 = T(0) = 5$ keV for $r_{cut} = 2r_c$. All the clusters are assumed to be detected above the same threshold of brightness. The dotted line is obtained assuming that $T_{weighted} = T_{obs}$.

are known, to estimate the emission-weighted temperature $T_{weighted}$ for each cluster in terms of eqs.(7) and (8), and the resultant $T_{weighted}$ versus T_{obs} is displayed in Fig.5. Now, it is straightforward to plot the emission-weighted temperature $T_{weighted}$ against the velocity dispersion σ for each of the 94 clusters (Fig.6). In our model a higher temperature cluster often exhibits a larger spatial extension in X-ray emission, in which the emission-weighted temperature over the whole cluster is smaller than T_c , while with the same detection threshold, the overall cluster temperature would appear to be higher than T_c if the cluster has a X-ray emitting region of radius $r < 1.25r_c$. This is the basic scenario illustrated in Fig.6. Employing the doubly weighted ODR method to the data set gives

$$\sigma = 10^{2.47 \pm 0.07} T^{0.67 \pm 0.07}, \quad (9)$$

Meanwhile, the average value β_{spec} according to σ and $T_{weighted}$ is $\beta_{spec} = 0.99 \pm 0.18$. These results are in good agreement with those found from the observed data. Of course, the real situation is much more complex. For examples, the absolute calibration of $r_{cut} = 2r_c$ for $T_0 = 5$ keV does not hold true for all the clusters selected with very different methods, and the kink at $T = 3.6$ keV in the simulated data has actually arisen from this poor calibration. Moreover, the flux threshold $S(r_{cut})$ does not remain to be constant in different observations, and it can be also affected by background emission. Although our analysis is only illustrative, it indeed shows that the nonisothermal intracluster gas can be one of the major reasons for the departure of the σ - T relationship from that expected under the scenario of isothermal hydrostatic equilibrium.

Fig. 6. The correlation between the emission-weighted temperature $T_{weighted}$ and the velocity dispersion σ for the 94 clusters in Fig. 2 (triangles). The solid line represents the best-fitted ODR σ - T relationship, $\sigma = 10^{2.47 \pm 0.07} T_{weighted}^{0.67 \pm 0.07}$. We also illustrate the isothermal case (squares) in which $T = T_c = (\mu m_p)\sigma^2$ (dotted line).

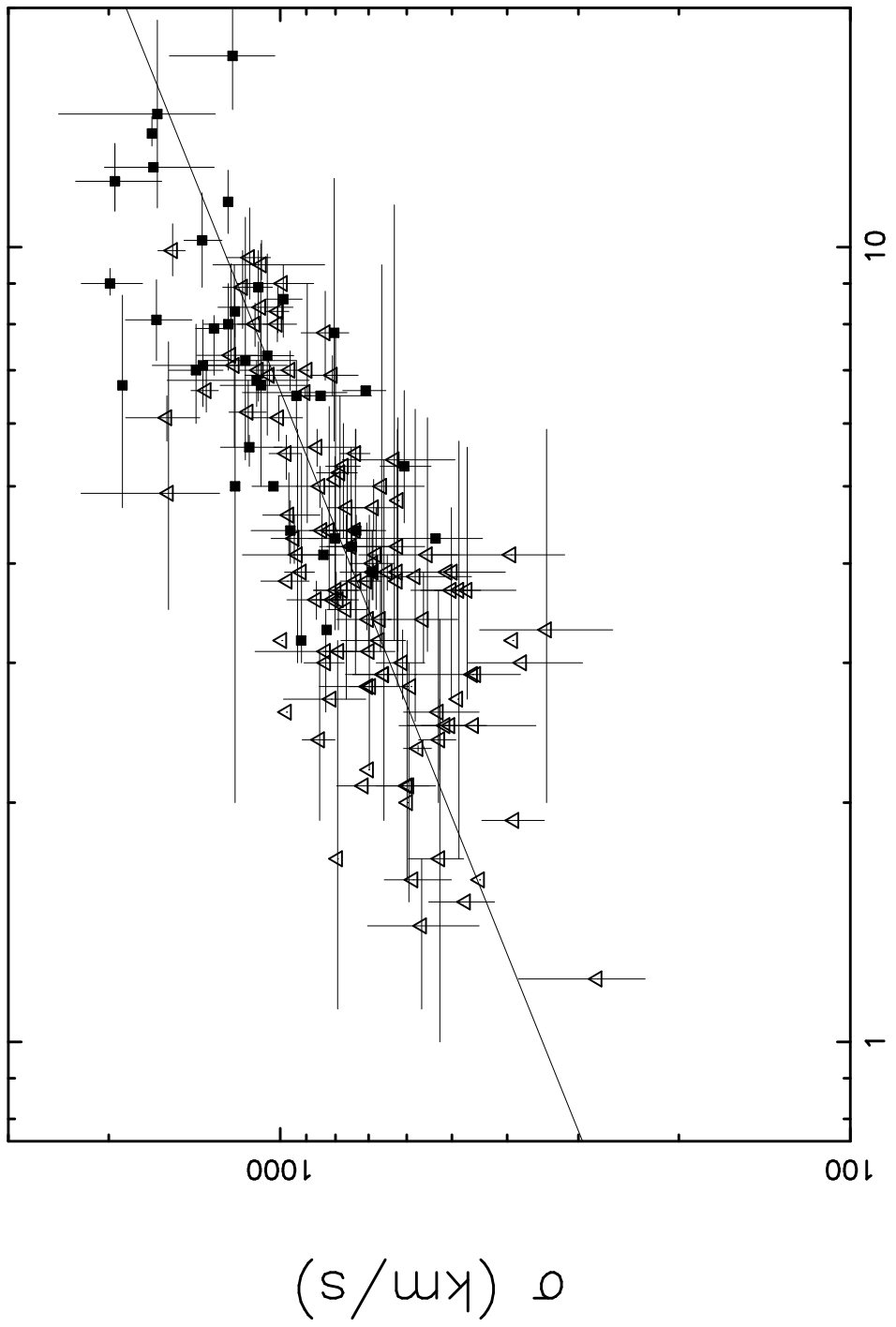
6. Conclusion

We have updated the σ - T relationship for clusters of galaxies using 149 published data sets of velocity dispersions and temperatures in literature, among which a subsample of 94 clusters is formed where measurement uncertainties in the two variables are known. These constitute the largest cluster samples ever used for such a kind of analysis. The previous claim that the fitted σ - T relationship is consistent with an isothermal hydrostatic scenario is found to have arisen from an inappropriate application of the OLS linear regression method. A plausible fit of the σ - T relationship has been achieved by using the doubly weighted ODR technique for a subsample of 94 clusters, which gives rise to $\sigma \propto T^{0.67 \pm 0.09}$. At a high significance level of $\sim 95\%$ we have detected a deviation of the σ - T relationship from that predicted by the isothermal and hydrostatic equilibrium model, though the mean value of the ratio β_{spec} between the specific energy of the galaxies and the gas is in excellent agreement with unity. We suggest that such a deviation may be due to the gas temperature decline at large cluster radius. This has been justified by a simple theoretical analysis, in which the gas temperature drop at large radius is described by a polytropic index of $\gamma = 1.3$. Yet, the real situation may be more complex than the nonisothermal temperature distribution for intracluster gas. A number of factors can also contribute to the reported deviation of σ - T relationship from $\sigma \propto T^{0.5}$ (Bird et al. 1995; Girardi et al. 1996; White et al. 1997)). Further work will thus be needed to explore the mechanism of this departure.

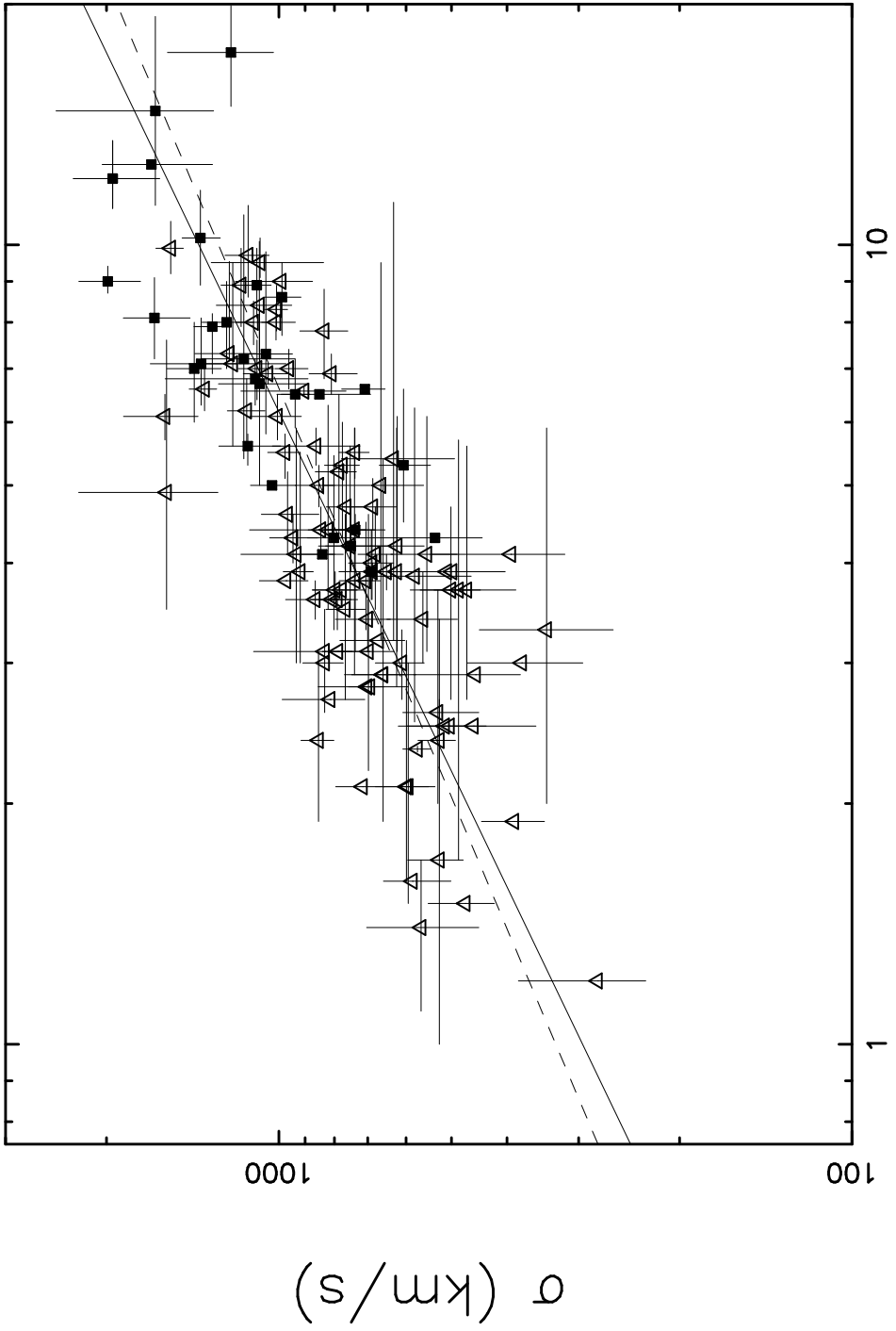
Acknowledgements. We thank the referee, David A. White, for many valuable suggestions and comments. This work was supported by the National Science Foundation of China, under Grant No. 19725311. Wen Xu acknowledges a World Laboratory fellowship.

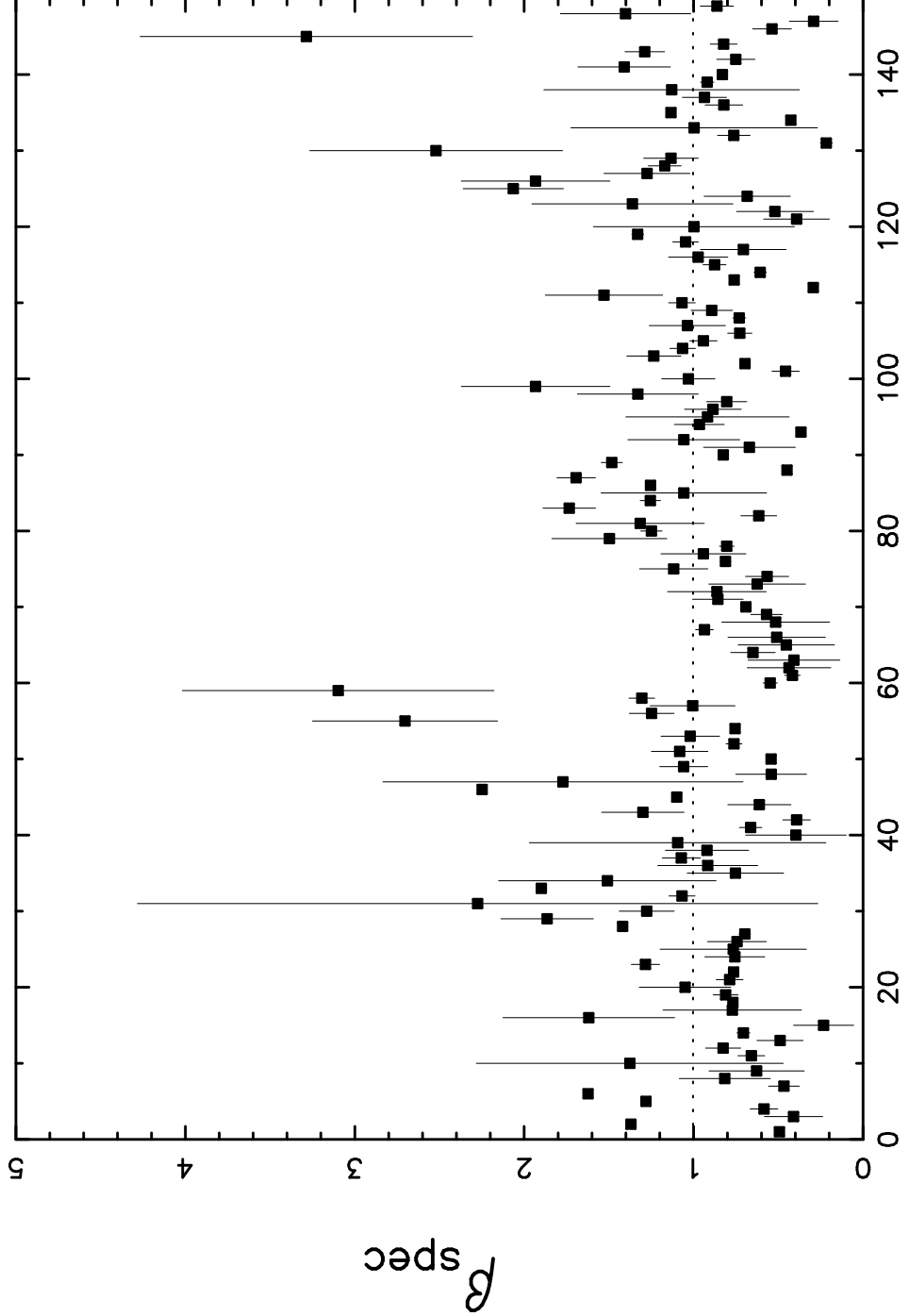
References

- Allen, S. W. 1998, MNRAS, in press
- Bahcall, N. A. & Cen, R. 1993, ApJ, 407, L49
- Bahcall, N. A. & Lubin, L. M. 1994, ApJ, 426, 513
- Bahcall, N. A., Lubin, L. M. & Dorman, V. 1995, ApJ, 447, L81
- Bird, C. M., Mushotzky, R. F. & Metzler, C. A. 1995, ApJ, 453, 40
- Bogg, P. T., Byrd, R. H., Donaldson, J. R., & Schnable, R. B. 1989, ACM Tran. Math. Software, 15, 348
- Bogg, P. T., & Rogers, J. E. 1990, Contem. Math., 112, 183
- Briel, U. G. & Henry, J. P. 1994, Nature, 372, 439
- Carlberg, R. G., et al. 1996, ApJ, 462, 32
- Carlberg, R. G., Yee, H. K. C. & Ellingson, E. 1997, ApJ, 478, 462
- Cavaliere, A. & Fusco-Femiano, R. 1976, A&A, 49, 137
- Chiueh, T. & Wu, X.-P. 1998, MNRAS, submitted
- Cowie, L. L., Henriksen, M. & Mushotzky, R. 1987, ApJ, 317, 593
- Ebeling, H., et al. 1996, MNRAS, 281, 799
- Edge, A. C. & Stewart, G. C. 1991, MNRAS, 252, 428
- Eke, V. R., Navarro, J. F. & Frenk, C. S. 1998, ApJ, in press
- Ettori, S., Fabian, A. C. & White, D. A. 1997, MNRAS, 289, 787
- Fadda, D., Girardi M., Giuricin, G., Mardirossian, F. & Mezzetti, M., 1996, ApJ, 473, 670
- Feigelson, E. D. & Babu, G. J. 1992, ApJ, 397, 55
- Gioia, I. M. & Luppino, G. A. 1994, ApJS, 94, 583
- Girardi M., Escalera, E., Fadda, D., Giuricin, G., Mardirossian, F. & Mezzetti, M. 1997, ApJ, 482, 41
- Girardi M., Fadda, D., Giuricin, G., Mardirossian, F. & Mezzetti, M. 1996, ApJ, 457, 61
- Henriksen, M., J. & White III, R. E. ApJ, 465, 515
- Isobe, T., Feigelson, E. D., Akritas, M. G. & Babu, G. J. 1990, ApJ, 364, 104
- Lubin, L. M. & Bahcall, N. A. 1993, ApJ, 415, L17
- Markevitch, M., Forman, W., R., Sarazin, C., L. & Vikhlinin, A. 1998, ApJ, in press
- Mushotzky, R. F. & Scharf, C. A. 1997, ApJ, 482, L13
- Ponman, T. J., Bourner, P. D. J., Ebeling, H. & Böhringer, H. 1996, MNRAS, 283, 690
- Rosati, P., Ceca, R. D., Norman, C. & Giacconi, R. 1998, ApJ, 492, L21
- Sadat, R., Blanchard, A. & Oukbir, J. 1998, A&A, 329, 21
- Smail, I., et al. 1997, ApJ, 479, 70
- Smith, B. W., Mushotzky, R. F. & Serlemitsos, P. J. 1979, ApJ, 227, 37
- Struble, M. F. & Rood, H. J. 1991, ApJS, 77, 363
- Vikhlinin, A., et al. 1998, ApJ, in press
- White, D. A. & Fabian, A. C. 1995, MNRAS, 273, 72
- White, D. A., Jones, C., Forman, W., 1997, MNRAS, 292, 419
- Wu, X.-P., Chiueh, Z., Fang, L.-Z. & Xue, Y.-J. 1998, MNRAS, in press
- Wu, X.-P. & Fang, L.-Z. 1997, ApJ, 483, 62
- Zabludoff, A., I., Huchra J. P. & Geller, M. J. 1990, ApJS, 74,

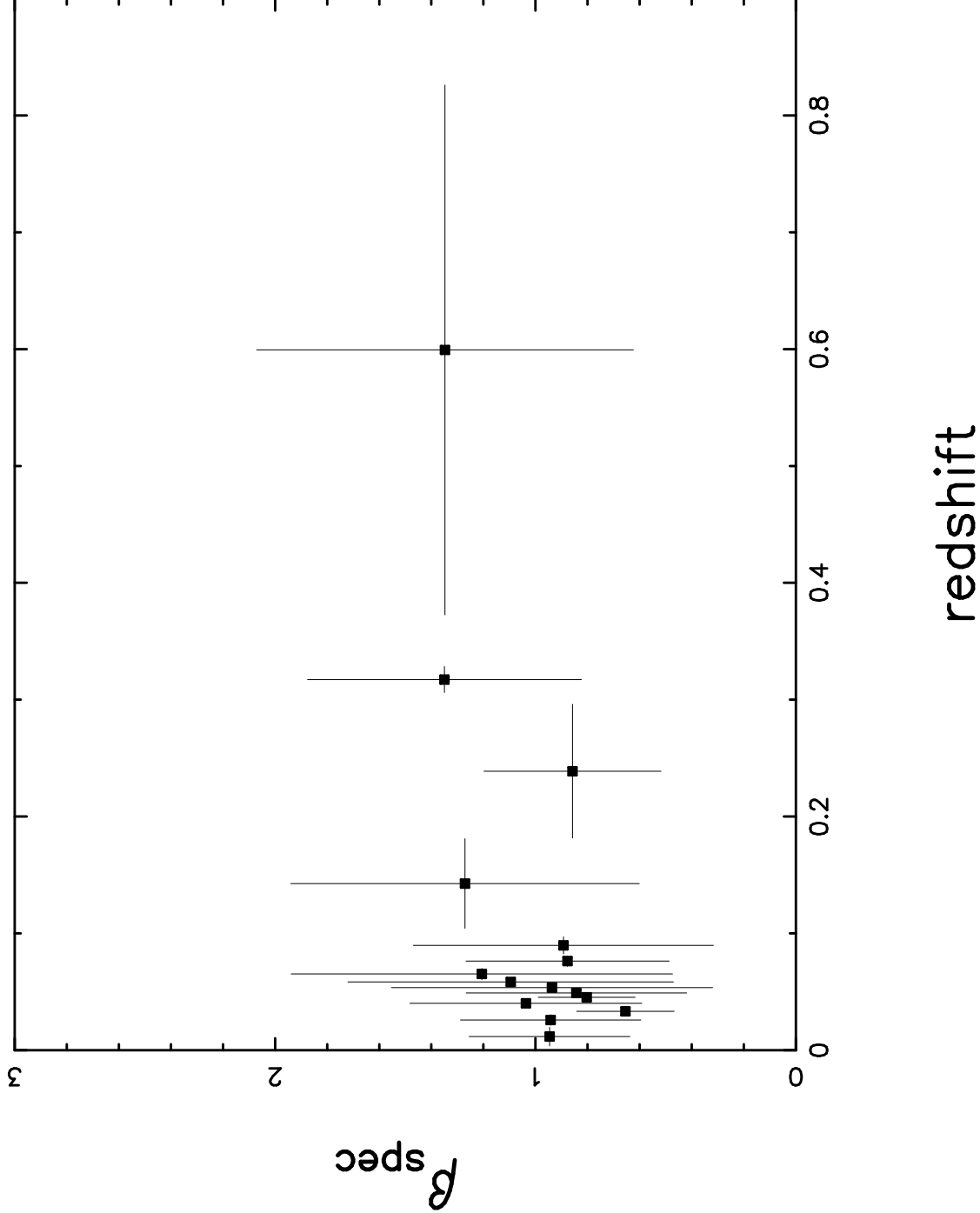


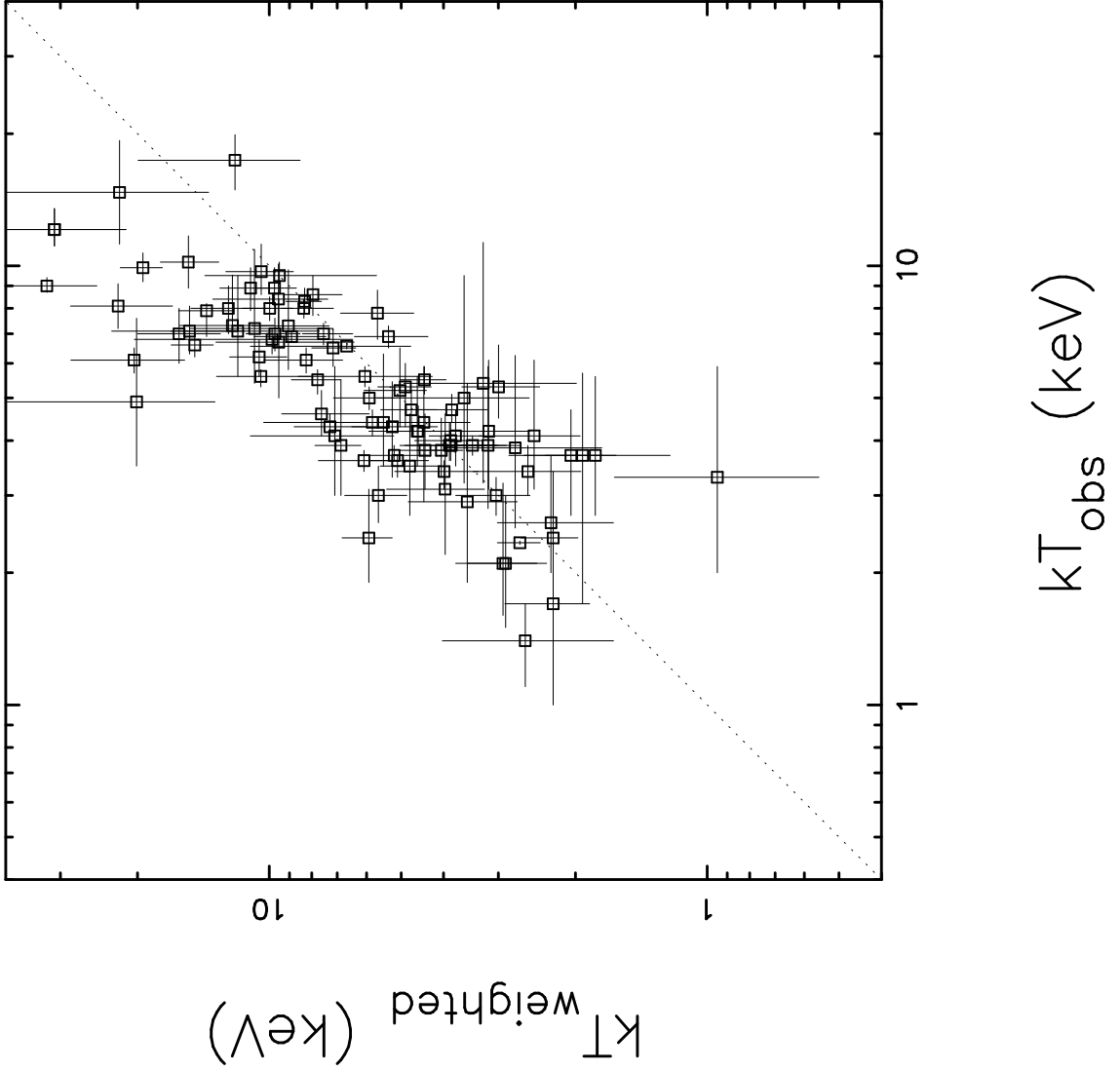
kT (keV)





measurement





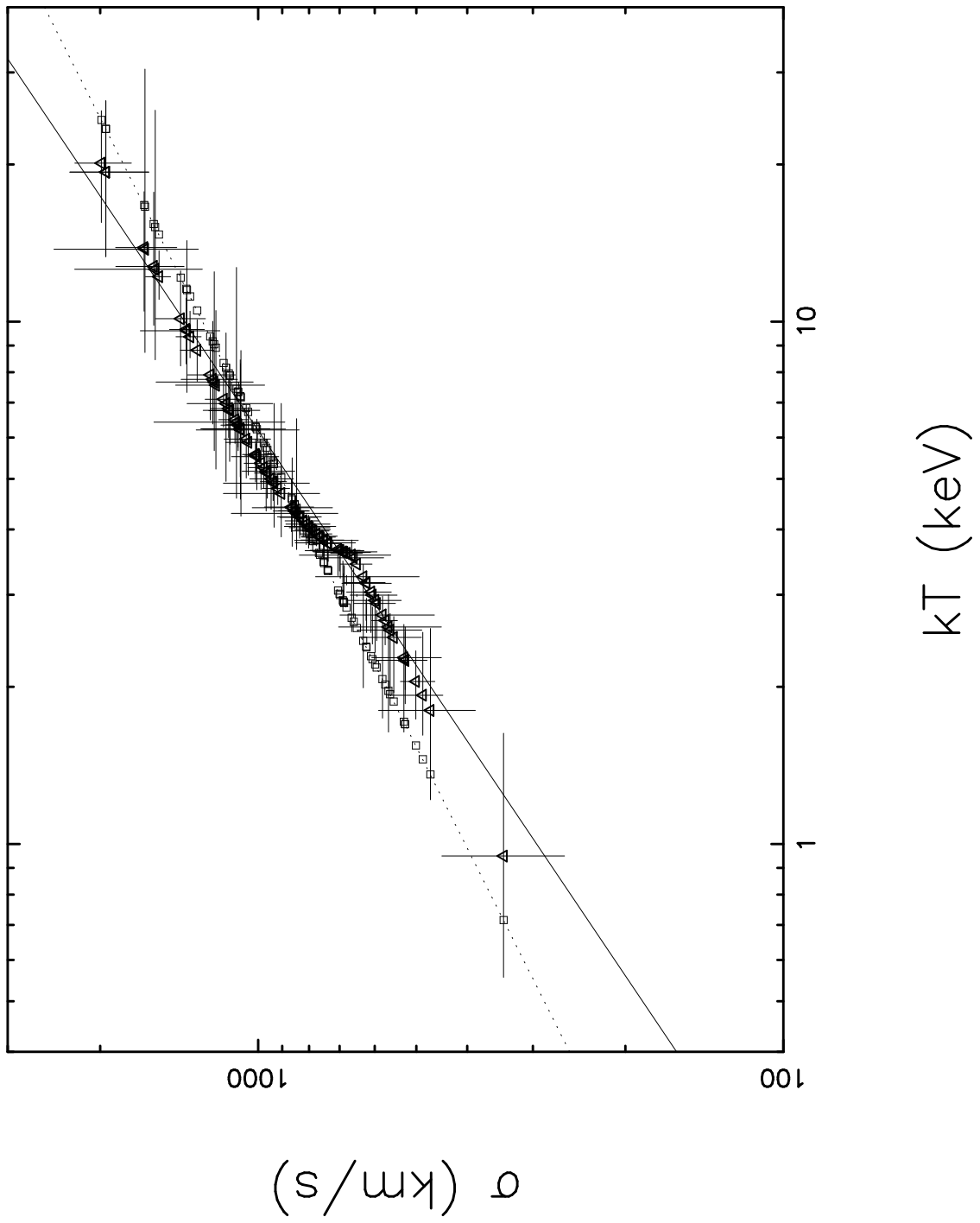


Table 1. Cluster Sample

cluster	redshift	T (keV)	σ (km/s)	β_{spec}
A21	0.0948	4.8	621	0.49
A74	0.0672	2.2	700	1.37
A77	0.0719	3.9	510^{+107}_{-107}	0.41 ± 0.17
A85	0.0559	$6.9^{+0.4}_{-0.4}$	810^{+76}_{-80}	0.58 ± 0.08
A98N	0.1043	3.3	829	1.28
A98S	0.1063	3.2	919	1.62
A115	0.1971	6.6	708^{+69}_{-55}	0.47 ± 0.09
A119	0.0443	$5.1^{+0.8}_{-0.6}$	862^{+165}_{-140}	0.82 ± 0.27
A133	0.0604	$3.8^{+1.7}_{-0.8}$	623	0.63 ± 0.28
A154	0.0652	3.1	833^{+274}_{-140}	1.38 ± 0.91
A168	0.0438	$2.6^{+1.1}_{-0.6}$	528^{+80}_{-80}	0.66 ± 0.08
A193	0.0490	$4.2^{+1.4}_{-0.7}$	751^{+78}_{-64}	0.83 ± 0.10
A194	0.0184	1.9	389^{+54}_{-45}	0.48 ± 0.17
A262	0.0169	$2.4^{+0.3}_{-0.2}$	525^{+47}_{-33}	0.71 ± 0.04
A367	0.0882	4.1	394^{+150}_{-77}	0.23 ± 0.18
A370	0.3730	$7.1^{+1.0}_{-0.8}$	1367^{+310}_{-184}	1.62 ± 0.51
A376	0.0489	$5.1^{+2.7}_{-1.6}$	800	0.77 ± 0.41
A397	0.0325	1.6	447	0.77
A399	0.0718	$5.8^{+0.8}_{-0.7}$	961^{+55}_{-71}	0.81 ± 0.07
A400	0.0237	$2.1^{+1.1}_{-0.5}$	599^{+80}_{-65}	1.05 ± 0.27
A401	0.0737	$8.0^{+0.4}_{-0.4}$	1012^{+60}_{-76}	0.79 ± 0.08
A407	0.0472	2.8	590	0.76
A426	0.0179	$6.2^{+0.6}_{-0.6}$	1138^{+92}_{-80}	1.28 ± 0.08
A458	0.1054	4.4	736^{+86}_{-58}	0.76 ± 0.18
A478	0.0881	$6.8^{+0.9}_{-0.8}$	904^{+261}_{-140}	0.77 ± 0.43
A496	0.0325	$3.9^{+0.1}_{-0.1}$	687^{+89}_{-76}	0.74 ± 0.17
A520	0.2010	$8.6^{+0.9}_{-0.9}$	988^{+76}_{-73}	0.70 ± 0.03
A539	0.0284	$3.0^{+0.5}_{-0.4}$	832^{+77}_{-60}	1.42 ± 0.03
A548	0.0415	$2.4^{+0.7}_{-0.5}$	853^{+62}_{-51}	1.86 ± 0.27
A576	0.0384	$4.3^{+0.3}_{-0.3}$	945^{+93}_{-88}	1.28 ± 0.16
A578	0.0864	$1.7^{+1.5}_{-0.6}$	793	2.28 ± 2.0
A665	0.1816	$8.3^{+0.6}_{-0.6}$	1201	1.07 ± 0.08
A671	0.0494	3.2	994	1.90
A744	0.0732	2.7	814^{+173}_{-106}	1.51 ± 0.64
A754	0.0535	$9.5^{+0.7}_{-0.4}$	1079^{+234}_{-243}	0.75 ± 0.28
A779	0.0230	1.5	473^{+76}_{-52}	0.92 ± 0.29
A851	0.4510	$6.7^{+1.7}_{-1.7}$	1081^{+194}_{-194}	1.07 ± 0.11
A957	0.0440	2.9	659^{+88}_{-56}	0.92 ± 0.25
A963	0.2060	$6.8^{+0.4}_{-0.5}$	1100^{+480}_{-210}	1.09 ± 0.87
A999	0.0317	1.2	278^{+104}_{-49}	0.40 ± 0.30
A1060	0.0126	$3.9^{+0.2}_{-0.2}$	649^{+49}_{-42}	0.66 ± 0.07
A1142	0.0350	$3.7^{+2.0}_{-2.0}$	486^{+81}_{-41}	0.39 ± 0.08
A1146	0.1422	5.0	1028^{+93}_{-96}	1.30 ± 0.24
A1185	0.0314	$3.9^{+2.0}_{-1.1}$	623^{+64}_{-50}	0.61 ± 0.19
A1213	0.0468	2.0	598	1.10
A1291	0.0530	2.6	975	2.25
A1300	0.3071	$5.0^{+3.0}_{-3.0}$	1200	1.77 ± 1.06
A1314	0.0329	$5.0^{+4.5}_{-1.8}$	664^{+171}_{-105}	0.54 ± 0.21

Table 1—Continued

cluster	redshift	T (keV)	σ (km/s)	β_{spec}
A1367	0.0214	$3.7^{+0.2}_{-0.1}$	798^{+75}_{-68}	1.06 ± 0.14
A1377	0.0514	2.7	488	0.54
A1631	0.0464	2.8	702^{+54}_{-46}	1.08 ± 0.17
A1644	0.0467	$4.7^{+0.5}_{-0.5}$	763^{+64}_{-50}	0.76 ± 0.05
A1651	0.0825	$6.1^{+0.4}_{-0.4}$	1006^{+118}_{-92}	1.02 ± 0.17
A1656	0.0231	$8.3^{+0.6}_{-0.5}$	1010^{+51}_{-44}	0.76 ± 0.02
A1689	0.1810	$9.0^{+0.4}_{-0.3}$	1989^{+245}_{-245}	2.70 ± 0.55
A1736	0.0431	$4.6^{+0.6}_{-0.5}$	966^{+107}_{-114}	1.25 ± 0.13
A1750	0.0855	3.7	778^{+97}_{-71}	1.01 ± 0.25
A1767	0.0700	$4.1^{+1.8}_{-1.1}$	933^{+232}_{-134}	1.31 ± 0.08
A1775	0.0696	$4.9^{+2.7}_{-1.4}$	1571^{+666}_{-293}	3.10 ± 0.92
A1795	0.0631	$7.8^{+1.0}_{-1.0}$	834^{+85}_{-70}	0.55 ± 0.04
A1809	0.0789	$3.7^{+1.0}_{-1.0}$	501^{+55}_{-40}	0.42 ± 0.05
A1913	0.0527	2.9	454^{+128}_{-75}	0.44 ± 0.25
A1940	0.1384	4.3	534^{+177}_{-92}	0.41 ± 0.27
A1983	0.0452	2.5	514^{+52}_{-43}	0.65 ± 0.13
A1991	0.0586	$5.4^{+5.9}_{-2.2}$	631^{+147}_{-137}	0.45 ± 0.28
A2009	0.1530	$7.8^{+4.4}_{-2.1}$	804	0.51 ± 0.29
A2029	0.0765	$8.9^{+1.0}_{-1.0}$	1164^{+98}_{-78}	0.94 ± 0.05
A2040	0.0456	2.5	458^{+141}_{-102}	0.52 ± 0.32
A2052	0.0348	$3.4^{+0.5}_{-0.4}$	561^{+87}_{-73}	0.57 ± 0.09
A2063	0.0355	$4.1^{+0.6}_{-0.6}$	679^{+49}_{-46}	0.69 ± 0.00
A2065	0.0722	$8.4^{+1.7}_{-1.2}$	1082^{+204}_{-132}	0.86 ± 0.15
A2079	0.0656	3.2	670^{+113}_{-67}	0.86 ± 0.29
A2092	0.0670	2.5	504^{+115}_{-69}	0.62 ± 0.29
A2107	0.0421	$4.2^{+1.9}_{-1.1}$	622^{+71}_{-64}	0.57 ± 0.13
A2124	0.0654	3.6	809^{+73}_{-60}	1.12 ± 0.20
A2142	0.0899	$9.7^{+1.5}_{-1.1}$	1132^{+110}_{-92}	0.81 ± 0.03
A2147	0.0356	$4.4^{+1.9}_{-0.9}$	821^{+68}_{-55}	0.94 ± 0.25
A2151	0.0370	$3.8^{+0.7}_{-0.5}$	705^{+46}_{-39}	0.80 ± 0.04
A2152	0.0374	2.1	715^{+81}_{-61}	1.50 ± 0.34
A2163	0.2030	$13.9^{+0.7}_{-0.5}$	1680	1.25 ± 0.06
A2197	0.0305	1.6	585^{+72}_{-84}	1.32 ± 0.38
A2199	0.0299	$4.7^{+0.4}_{-0.3}$	686^{+88}_{-62}	0.62 ± 0.11
A2218	0.1710	$7.0^{+1.0}_{-1.0}$	1405^{+163}_{-145}	1.73 ± 0.15
A2244	0.0970	$7.1^{+2.4}_{-1.5}$	1204^{+232}_{-232}	1.26 ± 0.06
A2250	0.0654	2.8	694^{+160}_{-99}	1.06 ± 0.49
A2255	0.0808	$7.3^{+2.2}_{-0.1}$	1221^{+181}_{-126}	1.25 ± 0.01
A2256	0.0581	$6.6^{+0.4}_{-0.4}$	1348^{+86}_{-64}	1.69 ± 0.11
A2271	0.0568	2.9	460	0.45
A2319	0.0559	$9.9^{+0.8}_{-0.7}$	1545^{+95}_{-77}	1.48 ± 0.06
A2390	0.2279	$8.9^{+1.0}_{-0.8}$	1093^{+61}_{-61}	0.83 ± 0.00
A2440	0.0904	9.0	991^{+200}_{-117}	0.67 ± 0.27
A2554	0.1108	4.1	840^{+131}_{-68}	1.06 ± 0.33
A2589	0.0416	$3.7^{+1.9}_{-1.0}$	470^{+120}_{-84}	0.37 ± 0.00
A2593	0.0433	$3.1^{+1.5}_{-0.9}$	698^{+116}_{-69}	0.97 ± 0.15
A2626	0.0573	$2.9^{+2.5}_{-1.0}$	658^{+111}_{-81}	0.92 ± 0.48
A2634	0.0309	$3.4^{+0.2}_{-0.3}$	700^{+97}_{-61}	0.89 ± 0.17

Table 1—Continued

cluster	redshift	T (keV)	σ (km/s)	β_{spec}
A2657	0.0414	$3.4^{+0.5}_{-0.3}$	667	0.80 ± 0.12
A2670	0.0759	$3.9^{+1.6}_{-0.9}$	918^{+65}_{-47}	1.33 ± 0.36
A2744	0.3080	$12.1^{+1.4}_{-1.0}$	1950^{+334}_{-334}	1.93 ± 0.44
A2877	0.0248	$3.5^{+1.1}_{-0.8}$	766^{+62}_{-59}	1.03 ± 0.16
A3112	0.0746	$4.1^{+2.0}_{-1.0}$	552^{+86}_{-63}	0.46 ± 0.08
A3122	0.0605	$5.3^{+0.7}_{-1.0}$	775^{+58}_{-51}	0.70 ± 0.03
A3128	0.0604	3.1	789^{+51}_{-44}	1.23 ± 0.16
A3158	0.0575	$5.5^{+0.4}_{-0.5}$	976^{+70}_{-58}	1.07 ± 0.08
A3266	0.0594	$8.0^{+0.5}_{-0.5}$	1107^{+82}_{-65}	0.94 ± 0.08
A3376	0.0490	$4.0^{+0.4}_{-0.4}$	688^{+68}_{-57}	0.73 ± 0.07
A3389	0.0267	$2.1^{+0.9}_{-0.6}$	595^{+63}_{-47}	1.04 ± 0.22
A3391	0.0553	$5.2^{+1.3}_{-0.9}$	786^{+78}_{-53}	0.73 ± 0.04
A3395	0.0506	$5.0^{+0.3}_{-0.3}$	852^{+84}_{-53}	0.89 ± 0.12
A3526	0.0114	$3.6^{+0.1}_{-0.3}$	791^{+62}_{-62}	1.07 ± 0.08
A3528N	0.0553	3.8	972^{+110}_{-82}	1.53 ± 0.35
A3530	0.0532	3.2	391	0.29
A3532	0.0559	$4.4^{+1.5}_{-1.5}$	738^{+112}_{-85}	0.76 ± 0.03
A3558	0.0475	$3.8^{+1.0}_{-0.5}$	737^{+49}_{-41}	0.61 ± 0.04
A3562	0.0478	$3.8^{+0.8}_{-0.7}$	736^{+49}_{-36}	0.88 ± 0.07
A3571	0.0396	$6.9^{+0.2}_{-0.2}$	1045^{+109}_{-90}	0.97 ± 0.17
A3627	0.0155	$7.0^{+2.0}_{-2.5}$	897	0.71 ± 0.08
A3667	0.0566	$7.0^{+0.6}_{-0.6}$	1092^{+86}_{-70}	1.05 ± 0.08
A3888	0.1680	$7.9^{+0.3}_{-1.0}$	1307^{+100}_{-92}	1.33 ± 0.04
A4059	0.0478	$4.4^{+0.3}_{-0.3}$	845^{+280}_{-140}	1.00 ± 0.59
A4067	0.0959	3.9	499^{+123}_{-74}	0.39 ± 0.19
1E0657	0.2960	$17.4^{+2.5}_{-2.5}$	1213^{+352}_{-191}	0.52 ± 0.23
3C295	0.4600	12.6	1670^{+364}_{-364}	1.36 ± 0.59
AC103	0.3100	6.5	850^{+158}_{-158}	0.68 ± 0.25
AC114	0.3100	$8.1^{+1.0}_{-0.9}$	1649^{+220}_{-220}	2.07 ± 0.30
AC118	0.3080	$12.1^{+1.4}_{-1.0}$	1950^{+334}_{-334}	1.93 ± 0.44
AWM7	0.0176	$3.6^{+0.2}_{-0.2}$	864^{+110}_{-80}	1.28 ± 0.25
CL0016+16	0.5545	$8.0^{+1.0}_{-1.0}$	1234^{+128}_{-128}	1.17 ± 0.10
CL0500–24	0.3270	7.2	1152^{+214}_{-214}	1.13 ± 0.42
Cygnus-A	0.0570	$6.1^{+0.4}_{-0.4}$	1581^{+286}_{-197}	2.52 ± 0.75
Klemola 44	0.0276	$3.3^{+2.6}_{-1.3}$	341^{+106}_{-80}	0.22 ± 0.04
MKW 3S	0.0434	$3.0^{+0.3}_{-0.3}$	610^{+69}_{-52}	0.76 ± 0.10
MKW 4	0.0198	$1.7^{+1.7}_{-0.7}$	525^{+71}_{-48}	1.00 ± 0.73
MS0440+02	0.1965	$5.3^{+1.3}_{-0.8}$	606^{+62}_{-62}	0.43 ± 0.02
MS0451–03	0.5392	$10.2^{+1.5}_{-1.3}$	1371^{+105}_{-105}	1.13 ± 0.01
MS0839+29	0.1928	$4.2^{+0.6}_{-0.3}$	749^{+104}_{-104}	0.82 ± 0.11
MS1008–12	0.3062	$7.3^{+2.5}_{-1.5}$	1054^{+107}_{-107}	0.94 ± 0.13
MS1054–03	0.8260	$14.7^{+4.6}_{-3.5}$	1643^{+806}_{-343}	1.13 ± 0.75
MS1224+20	0.3255	$4.3^{+1.15}_{-1.0}$	802^{+90}_{-90}	0.92 ± 0.04
MS1358+62	0.3283	$6.5^{+0.7}_{-0.6}$	937^{+54}_{-54}	1.00 ± 0.01
MS1455+22	0.2570	$5.6^{+0.2}_{-0.3}$	1133^{+140}_{-140}	1.41 ± 0.27
MS1512+36	0.3726	$3.9^{+0.5}_{-0.3}$	690^{+96}_{-96}	0.75 ± 0.11
MS2137–23	0.3130	$4.4^{+0.4}_{-0.4}$	960	1.29 ± 0.12
RXJ1347–114	0.4510	$11.4^{+1.1}_{-1.0}$	1235	0.82 ± 0.08

Table 1—Continued

cluster	redshift	T (keV)	σ (km/s)	β_{spec}
RXJ1716+67	0.813	$6.7^{+2.0}_{-2.0}$	1892	3.29 ± 0.98
S0805	0.0141	$1.4^{+0.3}_{-0.3}$	541^{+57}_{-43}	1.40 ± 0.38
SC1327–312	0.0495	$3.9^{+2.4}_{-1.3}$	580^{+119}_{-118}	0.54 ± 0.11
SC1329–31	0.0499	3.0	377^{+93}_{-82}	0.29 ± 0.14
Virgo	0.0038	$2.34^{+0.02}_{-0.02}$	573^{+35}_{-30}	0.86 ± 0.10

Table 2. Summary of the best fitted σ - T relationships

authors	No.	method	fitted relation	β_{spec}
Smith et al. (1979)	13	OLS(unweighted) ^a	$\sigma = 10^{2.78 \pm 0.08} T^{0.31 \pm 0.11}$	1.24 ± 0.18
Edge & Stewart (1991)	23	OLS(unweighted)	$\sigma = 10^{2.61 \pm 0.06} T^{0.45 \pm 0.09}$	0.91 ± 0.38
		Bisector(weighted)	$\sigma = 10^{2.41 \pm 0.51} T^{0.75 \pm 0.08}$	
Lubin & Bahall (1993)	41	OLS(weighted)	$\sigma = 10^{2.60 \pm 0.07} T^{0.50 \pm 0.11}$	1.14 ± 0.57
		Bisector(weighted)	$\sigma = 10^{2.36 \pm 0.05} T^{0.87 \pm 0.08}$	
Bird et al. (1995)	22	OLS(unweighted)	$\sigma = 10^{2.62 \pm 0.07} T^{0.42 \pm 0.11}$	0.90 ± 0.37
		Bisector(weighted)	$\sigma = 10^{2.50 \pm 0.09} T^{0.61 \pm 0.13}$	
Girardi et al. (1996)	37	ORD(weighted)	$\sigma = 10^{2.53 \pm 0.04} T^{0.61 \pm 0.05}$	1.03 ± 0.29
Ponman et al. (1996) ^b	27	OLS(unweighted) ^a	$\sigma = 10^{2.54 \pm 0.04} T^{0.55 \pm 0.05}$	0.88 ± 0.36
Wu & Fang (1997) ^c	17	OLS(unweighted)	$\sigma = 10^{2.64 \pm 0.11} T^{0.51 \pm 0.13}$	1.29 ± 0.71
White et al. (1997) ^d	83	OLS(unweighted) ^a	$\sigma = 10^{2.60 \pm 0.04} T^{0.49 \pm 0.06}$	1.06 ± 0.51
		ORD(weighted)	$\sigma = 10^{2.53 \pm 0.08} T^{0.60 \pm 0.10}$	1.15 ± 0.57
This work	149	OLS(unweighted)	$\sigma = 10^{2.54 \pm 0.03} T^{0.56 \pm 0.04}$	1.00 ± 0.52
		ORD(unweighted)	$\sigma = 10^{2.47 \pm 0.03} T^{0.67 \pm 0.04}$	
		ORD(weighted)	$\sigma = 10^{2.47 \pm 0.06} T^{0.67 \pm 0.09}$	1.00 ± 0.49

^aFitted by this work;

^bIncluding 17 Hickson’s compact galaxy groups;

^cThe gravitational lensing clusters in which arclike images are detected;

^dWe have only used the clusters whose σ and T are observationally determined;

^eUncertainties in two variables are known.